

# Scattering by a reflectionless modified Pöschl-Teller potential: Bohmian trajectories and arrival times

S. V. Mousavi<sup>1,2,\*</sup>

<sup>1</sup>*Department of Physics, The University of Qom, P. O. Box 37165, Qom, Iran*

<sup>2</sup>*School of Physics, Institute for Research in Fundamental Sciences (IPM), P.O.Box 19395-5531, Tehran, Iran*

A nonreflecting wavepacket is constructed by the superposition of reflectionless eigenstates of sech<sup>2</sup> potential. Free propagation and propagation in the presence of the above potential of such a wavepacket is considered using the concept of arrival time. Comparison is made with the free evolving Gaussian wavepacket. Mean arrival time at a detector behind the well is given as a function of mass for separate cases. A selection of Bohmian trajectories in the interacting case are computed and compared to the trajectories of a free particle guided by a Gaussian packet.

PACS numbers: 03.65.-w, 03.65.Nk, 03.65.Ta

Keywords: Reflectionless potential, Nonreflecting wavepacket, Arrival time, Bohmian trajectory

## I. INTRODUCTION

Scattering of incident waves by inhomogeneities is a common physical feature in optics and quantum mechanics. The trigonometric Pöschl-Teller (PT) potential was suggested by Pöschl and Teller [1] to describe diatomic molecular vibration. PT-type potentials have been noticed by authors from different areas of physics ranging from the molecular physics to the nuclear one. Using different approximation methods, analytical solutions of the Schrödinger equation and energy eigenvalues for diatomic molecules have been found for the trigonometric PT molecular potential [2]. Approximate bound-state solutions of the Klein-Gordon [3] and Dirac [4] equations with such potentials have been investigated. The Sech-squared potential (or Modified PT potential) has attracted too much attention, for instance it appears in the context of neutron-matter [5] and spherical quantum dot [6].

There are obstacles, called reflectionless potentials, which are completely transparent for the incident wave. This type of potentials have been extensively studied analytically and numerically in the literature. Using the method of summation over eigenstates, the exact propagator for a general reflectionless potential has been computed [7]. Scattering of a Gaussian wavepacket by a reflectionless sech<sup>2</sup> potential has been numerically studied and possible applications of such potentials has been argued [8]. It has been shown that in comparison to the case of free evolution, the wavepacket accelerates in the well and is narrower. Authors arrived at this result by plotting the probability density versus position in a time that the whole wavepacket has left the well. In this paper we employ the concept of arrival time [9] for quantitative study of this problem. In the case of reflectionless sech<sup>2</sup> potential non-reflecting wavepackets have been constructed by superposing energy eigenstates and propagation of them has been studied in the presence of the above potential [10]. Similar results have been reproduced by the method of supersymmetric quantum mechanics [11]. Traversal time through the reflectionless sech<sup>2</sup> potential has been studied using the method of a quantum clock [12]. Only, recently, a true reflectionless potential was realized experimentally in photonic lattices using the concept of arrays of evanescently couple waveguides [13].

It seems to be interesting to consider the problem of a wavepacket scattering by the reflectionless Sech<sup>2</sup> potential using a trajectory-based theory, since by attributing a well-defined trajectory to a particle, its arrival time at a detector location is a well-defined and predictable quantity. It has been shown within the Bohmian mechanics [14] that the arrival time distribution is given by the probability current density [15]. But, there is no consensus about this quantity within the standard formulation of the quantum mechanics [16].

To this end, we at first follow Lekner [10] to construct a non-reflecting wavepacket. Then, propagation of such a constructed wavepacket is considered and arrival time at a detector location behind the well is computed. Comparison with a freely evolving Gaussian wavepacket is made. Finally, a selection of Bohmian paths is plotted.

---

\*Electronic address: vmousavi@qom.ac.ir

### A. Constructing a nonreflecting wavepacket

Exact solution of the Schrödinger equation for any positive energy  $E_k = \frac{\hbar^2 k^2}{2m}$  is given by

$$\psi_k(x) = A(k) \frac{ik - a \tanh(ax)}{ik + a} e^{ikx}, \quad (1)$$

in the presence of the sech<sup>2</sup> potential

$$V(x) = -\frac{\hbar^2 a^2}{2m} \frac{\nu(\nu+1)}{\cosh^2(ax)}, \quad (2)$$

with  $\nu = 1$ . One easily sees that in the limit  $x \rightarrow -\infty$ , the above solution reduces to  $A(k)e^{ikx}$ . This shows the nonreflectivity of the potential; with an incident wave from the left there is no reflected wave [17].

By superposing the reflectionless eigenstates (1), one obtains nonreflecting wavepacket

$$\Psi_{i,nr}(x, t) = \frac{1}{\sqrt{2\pi}} \int_{-\infty}^{\infty} dk \psi_k(x) e^{-iE_k t/\hbar}, \quad (3)$$

where sub-indices "i" and "nr" stand respectively for "interacting" and "nonreflecting". Noting the factor  $(ik + a)^{-1}$  in the relation of  $\psi_k(x)$ , a simple choice for  $A(k)$  is [10]

$$A(k) = (ik + a)\phi_0(k), \quad (4)$$

where,

$$\phi_0(k) = \left(\frac{2}{\pi}\sigma_0^2\right)^{1/4} e^{-\sigma_0^2(k-k_0)^2} e^{-i(k-k_0)x_c}, \quad (5)$$

is the Fourier transform of the initial Gaussian wavepacket

$$\Psi_G(x, 0) = \frac{1}{(2\pi\sigma_0^2)^{1/4}} \exp\left[-\frac{(x-x_c)^2}{4\sigma_0^2} + ik_0 x\right], \quad (6)$$

where subindex "G" stands for "Gaussian". Here,  $k_0$  is the kick momentum; and  $x_c$  and  $\sigma_0$  are respectively the center and rms width of the packet. Time-evolved Gaussian wavepacket in free space is given by,

$$\Psi_{f,G}(x, t) = \frac{1}{(2\pi s_t^2)^{1/4}} \exp\left[-\frac{(x-x_c-ut)^2}{4s_t\sigma_0} + ik_0\left(x - \frac{ut}{2}\right)\right], \quad s_t = \sigma_0\left(1 + i\frac{\hbar t}{2m\sigma_0^2}\right), \quad (7)$$

where  $s_t = \sigma_0(1 + i\hbar t/2m\sigma_0^2)$  and  $u = \hbar k_0/m$  is the group velocity of the packet. In this equation subindex "f" stands for "free".

By the choice (4) for  $A(k)$ , reflectionless wavepacket reads

$$\Psi_{i,nr}(x, t) = N \left[ ik_0 - \frac{x-x_c-ut}{2\sigma_0 s_t} - a \tanh(ax) \right] \Psi_{f,G}(x, t), \quad (8)$$

where  $N$ , which has the length dimension, shows the normalization constant.

Free evolution of the initial nonreflecting wavepacket  $\Psi_{nr}(x) = \Psi_{i,nr}(x, 0)$  is given by the integral relation

$$\Psi_{f,nr}(x, t) = \int_{-\infty}^{\infty} dx' G_f(x, t; x', 0) \Psi_{nr}(x'), \quad (9)$$

where,

$$G_f(x, t; x', 0) = \sqrt{\frac{m}{2\pi i \hbar t}} \exp\left\{\frac{im}{2\hbar t}(x-x')^2\right\},$$

represents the propagator of free particle. From eqs. (8) and (9) one obtains,

$$\Psi_{f,nr}(x, t) = N \left\{ ik_0 - \frac{x-x_c-ut}{2\sigma_0 s_t} - a \sqrt{\frac{m}{2\pi i \hbar t}} \frac{s_t}{\sigma_0} g(x, t) \right\} \Psi_{f,G}(x, t), \quad (10)$$

where,

$$g(x, t) = \int_{-\infty}^{\infty} dx' \tanh(ax') \exp \left\{ -\frac{im}{2\hbar t} \frac{s_t}{\sigma_0} \left[ x' - \frac{\sigma_0}{s_t} \left( x - ut + \frac{i\hbar t}{2m\sigma_0^2} x_c \right) \right]^2 \right\} .$$

Just for completeness we mention that the evolution of the Gaussian wavepacket (6) in the presence of the nonreflecting potential (2) with  $\nu = 1$  which has been numerically studied in [8], is given by

$$\Psi_{i,G}(x, t) = \int_{-\infty}^{\infty} dx' G_i(x, t; x', 0) \Psi_G(x', 0) , \quad (11)$$

where,

$$\begin{aligned} G_i(x, t; x', 0) &= G_f(x, t; x', 0) + \frac{\exp \left[ \frac{i\hbar t}{2m} a^2 \right]}{2 \cosh(ax) \cosh(ax')} \\ &\times \left\{ \operatorname{erf} \left( a \sqrt{\frac{i\hbar t}{2m}} - (x - x') \sqrt{\frac{m}{2i\hbar t}} \right) + \operatorname{erf} \left( a \sqrt{\frac{i\hbar t}{2m}} + (x - x') \sqrt{\frac{m}{2i\hbar t}} \right) \right\} , \end{aligned}$$

represents the propagator of the nonreflecting potential for  $\nu = 1$  [7, 18].

## II. BASIC EQUATIONS

Using eq. (8) probability density and probability current density becomes

$$\begin{aligned} \rho_{i,nr}(x, t) &= |N|^2 \left[ \left( k_0 + \frac{\hbar t(x - x_c - ut)}{4m\sigma_0^2\sigma_t^2} \right)^2 + \left( a \tanh(ax) + \frac{x - x_c - ut}{2\sigma_t^2} \right)^2 \right] \\ &\times \frac{1}{\sqrt{2\pi}\sigma_t} \exp \left[ -\frac{(x - x_c - ut)^2}{2\sigma_t^2} \right] , \end{aligned} \quad (12)$$

and

$$j_{i,nr}(x, t) = |N|^2 \frac{m\sigma_0\hbar\sqrt{\frac{2}{\pi}} \left( f_3(x) m^3 + f_2(x, t) m^2 + f_1(x, t) m + f_0(x, t) \right)}{(2m\sigma_0\sigma_t)^5} \exp \left[ -\frac{(x - x_c - ut)^2}{2\sigma_t^2} \right] , \quad (13)$$

where  $\sigma_t = |s_t| = \sigma_0 \sqrt{1 + \frac{\hbar^2 t^2}{4m^2\sigma_0^4}}$  and

$$\begin{aligned} f_3(x) &= 4 \left[ 4k_0^3\sigma_0^8 + k_0\sigma_0^4(2\sigma_0^2 + 4a^2\sigma_0^4 + (x - x_c)^2) + 4ak_0\sigma_0^6(x - x_c) \tanh(ax) \right] , \\ f_2(x, t) &= 4\hbar t \left[ a^2\sigma_0^4(x - x_c) + k_0^2\sigma_0^4(x - x_c) - a\sigma_0^2(\sigma_0^2 + 4k_0^2\sigma_0^4 - (x - x_c)^2) \tanh(ax) + (x - x_c)^3 \right] , \\ f_1(x, t) &= \hbar^2 t^2 \left[ 2k_0\sigma_0^2(1 + 2a^2\sigma_0^2) - 4ak_0\sigma_0^2(x - x_c) \tanh(ax) \right] , \\ f_0(x, t) &= a\hbar^3 t^3 \left[ a(x - x_c) - \tanh(ax) \right] . \end{aligned}$$

According to the Ehrenfest theorem, expectation value of momentum remains unchanged in the free space. Thus, in the free space one has

$$\langle x \rangle(t) = \langle x \rangle(0) + \frac{\langle p \rangle(0)}{m} t . \quad (14)$$

For the freely evolving Gaussian wavepacket this equation reads,

$$\langle x \rangle_{f,G}(t) = x_c + ut . \quad (15)$$

In the Bohmian view of the world, the state of a system is described by its wave function together with its actual configuration defined by the actual position of its particle. In the minimal approach to the theory [19], particle equation of motion, known as guidance equation, is

$$v(x, t) = \frac{j(x, t)}{\rho(x, t)} = \frac{\hbar}{m} \Im \frac{\nabla \psi}{\psi} . \quad (16)$$

Using this equation and eqs. (12) and (13), one obtains

$$v_{\text{nr}}(x, 0) = u \frac{1}{16\sigma_0^8 k_0} \frac{f_3(x)}{k_0^2 + \left(a \tanh(ax) + \frac{x-x_c}{2\sigma_0^2}\right)^2} , \quad (17)$$

for the initial Bohmian velocity of a particle which is guided by the nonreflecting wave packet (8). It is clear from eq. (17) that initial velocity depends on the position in the nonreflecting wavepacket case, while it is constant value  $u$  for the Gaussian packet. By integrating guidance equation (16) over time one obtains

$$x_{\text{f,G}}(t) = x_c + ut + \frac{\sigma_t}{\sigma_0} (x_0 - x_c) , \quad (18)$$

for the trajectories of a free particle which is guided by the Gaussian packet (7). Here,  $x_0$  is the initial position of the particle.

Within the Bohmian mechanics, the arrival time distribution of particles at detector location  $x_d$  is given by [15]

$$\Pi(x_d, t) = \frac{|j(x_d, t)|}{\int_0^\infty dt |j(x_d, t)|} , \quad (19)$$

and thus the mean arrival time reads

$$\tau(x_d) = \int_0^\infty dt t \Pi(x_d, t) . \quad (20)$$

### III. SCALING THE UNIT OF LENGTH

In order to do numerical calculations, we apply a scaling transformation which eliminates physical constant  $\hbar$  and mass  $m$  in the Schrödinger equation for free particle and for a particle interacting with sech<sup>2</sup> potential (2). Wavefunction  $\Psi(x, t)$  which describes a particle of mass  $m$  in the potential (2) with  $\nu = 1$ , satisfies the Schrödinger equation

$$i\hbar \frac{\partial}{\partial t} \Psi(x, t) = \left( -\frac{\hbar^2}{2m} \frac{\partial^2}{\partial x^2} - \frac{\hbar^2 a^2}{m} \text{sech}^2(ax) \right) \Psi(x, t) . \quad (21)$$

By space transformation  $x \rightarrow \bar{x} = \sqrt{\frac{m}{\hbar}} x$ , which is a scaling of unit length [20], and defining new function

$$\bar{\Psi}(\bar{x}, t) = \Psi(\sqrt{\hbar/m} \bar{x}, t) , \quad (22)$$

Schrödinger equation (21) reads

$$i \frac{\partial}{\partial t} \bar{\Psi}(\bar{x}, t) = \left( -\frac{1}{2} \frac{\partial^2}{\partial \bar{x}^2} - \bar{a}^2 \text{sech}^2(\bar{a}\bar{x}) \right) \bar{\Psi}(\bar{x}, t) , \quad (23)$$

where  $\bar{a} = \sqrt{\frac{\hbar}{m}} a$ . Thus, transformed momentum operator is  $\bar{p} = -i\partial/\partial\bar{x}$ . Eq. (23) says that the above scale transformation corresponds to put  $\hbar = m = 1$  in the equations of section II.

Continuity equation becomes

$$\frac{\partial \bar{\rho}(\bar{x}, t)}{\partial t} + \frac{\partial \bar{j}(\bar{x}, t)}{\partial \bar{x}} = 0 , \quad (24)$$

where,

$$\begin{aligned}\bar{\rho}(\bar{x}, t) &= |\bar{\Psi}(\bar{x}, t)|^2, \\ \bar{j}(\bar{x}, t) &= \Im \left\{ \bar{\Psi}^*(\bar{x}, t) \frac{\partial}{\partial \bar{x}} \bar{\Psi}(\bar{x}, t) \right\},\end{aligned}\quad (25)$$

and thus, guidance equation in this new coordinate reads

$$\bar{v}(\bar{x}, t) = \frac{\bar{j}(\bar{x}, t)}{\bar{\rho}(\bar{x}, t)}. \quad (26)$$

In summary we have the following transformations,

$$\begin{aligned}x &\rightarrow \bar{x} = \sqrt{\frac{m}{\hbar}} x, \\ t &\rightarrow t, \\ p = -i\hbar\nabla &\rightarrow \bar{p} = -i\bar{\nabla} = \sqrt{\frac{1}{m\hbar}} p, \\ \rho(x, t) &\rightarrow \bar{\rho}(\bar{x}, t) = \rho(x, t), \\ j(x, t) &\rightarrow \bar{j}(\bar{x}, t) = \sqrt{\frac{m}{\hbar}} j(x, t), \\ \Pi(x_d, t) &\rightarrow \bar{\Pi}(\bar{x}_d, t) = \Pi(x_d, t), \\ v(x, t) &\rightarrow \bar{v}(\bar{x}, t) = \sqrt{\frac{m}{\hbar}} v(x, t).\end{aligned}\quad (27)$$

#### IV. NUMERICAL CALCULATIONS

For numerical calculations, transformed parameters of the potential and wavepacket are taken as  $\bar{a} = 1$ ,  $\bar{\sigma}_0 = 1$ ,  $\bar{x}_c = -10$ ,  $\bar{k}_0 = 1$ . In figure 1, we have plotted transformed probability density  $\bar{\rho}(\bar{x}, t)$  versus transformed space coordinate  $\bar{x}$  at six different instants. A gap at the center of the potential is seen in the plot of interacting nonreflecting wavepacket. With respect to the relation  $\bar{x}_d = \sqrt{m/\hbar} x_d$ , for a given width  $\delta\bar{x}$  of  $\bar{\rho}$ , corresponding width in  $x$  is proportional to the inverse of square root of mass. Thus, from the forth equation of eq. (27) it follows that by increasing the mass, the width of probability density decreases. With the above values for the parameters of the wavepacket one obtains by numerical integration  $N \simeq 2.25$  for the normalization constant in eq. (8),  $\langle \bar{p} \rangle_{\text{nr}}(0) = \langle \bar{\Psi}_{\text{nr}} | \bar{p} | \bar{\Psi}_{\text{nr}} \rangle(0) \simeq 1.2222$  and  $\langle \bar{x} \rangle_{\text{nr}}(0) = \langle \bar{\Psi}_{\text{nr}} | \bar{x} | \bar{\Psi}_{\text{nr}} \rangle(0) \simeq -10.4444$  for the initial nonreflecting wavepacket. Because of the relation  $\langle \bar{p} \rangle_{\text{nr}}(0) > \langle \bar{p} \rangle_{\text{G}}(0)$ , expectation value of space coordinate of the nonreflecting wavepacket,  $\langle \bar{x} \rangle_{\text{nr}}$ , in the free-space moves faster than the center of the Gaussian wavepacket. In addition, in the interacting case because potential is attractive, wavepacket moves faster when the wavepacket approaches the well. After, passing the potential it moves with constant velocity. See Fig. 2. It must be noted that potential is proportional to the inverse of mass. Thus, it is more attractive for low masses. So, wavepackets describing particles with low values of mass move faster in comparison to the large ones. As one sees in plot b) of figure 2 uncertainty in position,  $\Delta\bar{x} = \sqrt{\langle \bar{\Psi}_{\text{nr}} | \bar{x}^2 | \bar{\Psi}_{\text{nr}} \rangle - \langle \bar{\Psi}_{\text{nr}} | \bar{x} | \bar{\Psi}_{\text{nr}} \rangle^2}$ , is larger for the interacting nonreflecting wavepacket compared to the freely evolving Gaussian wavepacket.

In figure 3 we have plotted arrival time distribution (19) at the detector location  $\bar{x}_d = 2\bar{a}$ . Relation  $\bar{x}_d = \sqrt{m/\hbar} x_d$  means fixing  $x_d$  and changing  $\bar{x}_d$  corresponds to changing mass. From plots (a) and (b) of this figure it is found that the width-in-time of the arrival time distribution increases with  $\bar{x}_d$  (mass) in contrast to the width-in-space of the detection probability density  $\rho$  where width-in-space in a given time decreases with mass. Plot (c) of Fig. 3 shows the mean arrival time (20). In agreement with the previous findings,  $\bar{\tau}$  is the lowest for the interacting nonreflecting wavepacket while is the largest for the free Gaussian. For all types of packets mean arrival time increases with  $\bar{x}_d$  (mass).

Figure 4 represents a selection of Bohmian paths. In plot (a), trajectories (18) for the free Gaussian have been plotted, while in plot (c) trajectories are for a particle which is guided by the wavepacket  $\Psi_{\text{i,nr}}(x, t)$ . In agreement with plot (c) of Fig. 2, trajectories spread out more in the case of interacting nonreflecting packet. In plot (c) we have depicted  $\langle \bar{x} \rangle(t)$  and the Bohm path with initial position  $\langle \bar{x} \rangle_{\text{nr}}(0)$ . It is seen that the Bohm path overtakes the expectation value of space coordinate. Plot (d) represents initial Bohmian velocity (17) versus space coordinate  $\bar{x}$ . As one sees, velocity is higher for the interacting nonreflecting wavepacket compared to the free Gaussian.

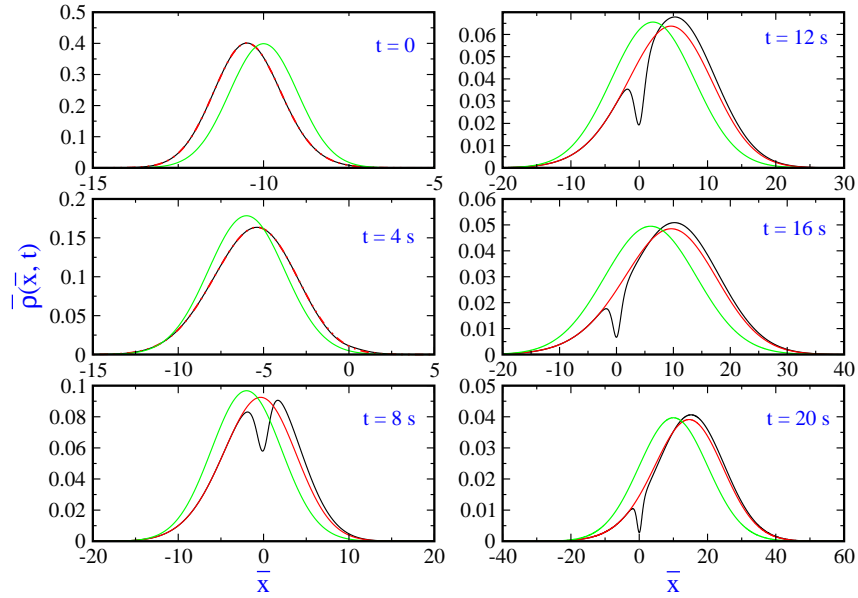


FIG. 1: (Color online) Transformed probability density  $\bar{\rho}(\bar{x}, t)$  versus transformed space coordinate  $\bar{x}$  at six different instants  $t = 0, t = 4 \text{ s}, t = 8 \text{ s}, t = 12 \text{ s}, t = 16 \text{ s}$  and  $t = 20 \text{ s}$ . In each plot black curve shows interacting nonreflecting wavepacket while the red one shows freely evolving nonreflecting packet and the green one stands for the propagation of free Gaussian packet.

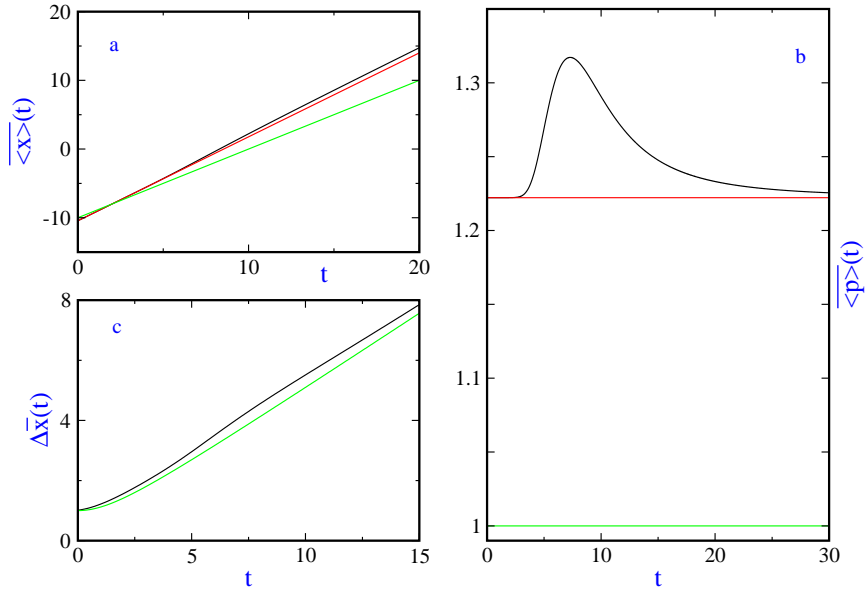


FIG. 2: (Color online) Expectation value of space coordinate and momentum (a and b); and uncertainty in position (c) with the same color scheme as in Fig. 1.

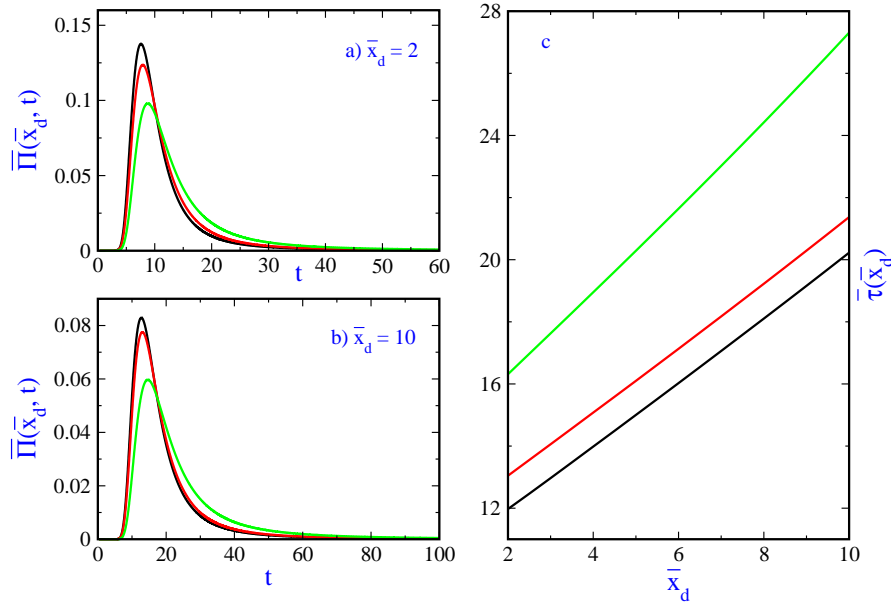


FIG. 3: (Color online) Arrival time distribution  $\bar{\Pi}(\bar{x}_d, t)$  versus time (left column) and mean arrival time  $\bar{\tau}(\bar{x}_d)$  versus detector position  $\bar{x}_d$  with the same color scheme as in Fig. 1.

## V. SUMMARY AND CONCLUSION

In this work we constructed a nonreflecting wavepacket by superposing of eigenstates of the reflectionless sech<sup>2</sup> potential. Then, evolution of this wavepacket in the presence of the potential and in free space studied and compared to the free propagation of Gaussian wavepacket. It was found that nonreflecting wavepacket moves faster and its width, uncertainty in position, is larger. Mean arrival time at a detector behind the well was computed as a function of mass. It was seen mean arrival time increases with mass in agreement with one's intuition and it is the largest for the free Gaussian compared to the nonreflecting wavepacket in free space and in the interacting case. Finally, a selection of Bohmian trajectories were computed.

- 
- [1] G. Pöschl and E. Teller, *Z. Physik* **83** (1933) 143.
  - [2] B. J. Falaye, *Can. J. Phys.* **90** (2012) 1259 and references therein.
  - [3] Wen-Chao Qiang and Shi-Hai Dong, *Phys. Lett. A* **372** (2008) 4789; Tao Chen, Yong-Feng Diao and Chun-Sheng Jia, *Phys. Scr.* **79** (2009) 065014.
  - [4] Ying Xu, Su He and Chun-Sheng Jia, *J. Phys. A: Math. Theor.* **41** (2008) 255302; Gao-Feng Wei and Shi-Hai Dong, *Eur. Phys. J. A* **43** (2010) 185.
  - [5] A. Gezerlis and J. Carlson, *Phys. Rev. C* **81** (2010) 025803.
  - [6] D.B. Hayrapetyan, E.M. Kazaryan and H.Kh. Tevosyan, *Superlattices and Microstructures* **64** (2013) 204.
  - [7] R. E. Crandall, *J. Math. Phys.* **16** (1983) 3005.
  - [8] N. Kiriushcheva and S. Kuzmin, *Am. J. Phys.* **66** (1998) 867.
  - [9] J. G. Muga and C. R. Leavens, *Phys. Rep* **338** (2000) 353.
  - [10] J. Lekner, *Am. J. Phys.* **75** (2007) 1151.
  - [11] T. Cox and J. Lekner, *Eur. J. Phys.* **29** (2008) 671.
  - [12] C-S. Park, *Phys. Lett. A* **375** (2011) 3348.
  - [13] A. Szameit, et.al, *Phys. Rev. Lett.* **106** (2011) 193903.
  - [14] D. Bohm and B. J. Hiley 1993, *The undivided universe* (London: Routledge);  
P. R. Holland 1993, *The Quantum Theory of Motion* (Cambridge: Cambridge University Press).

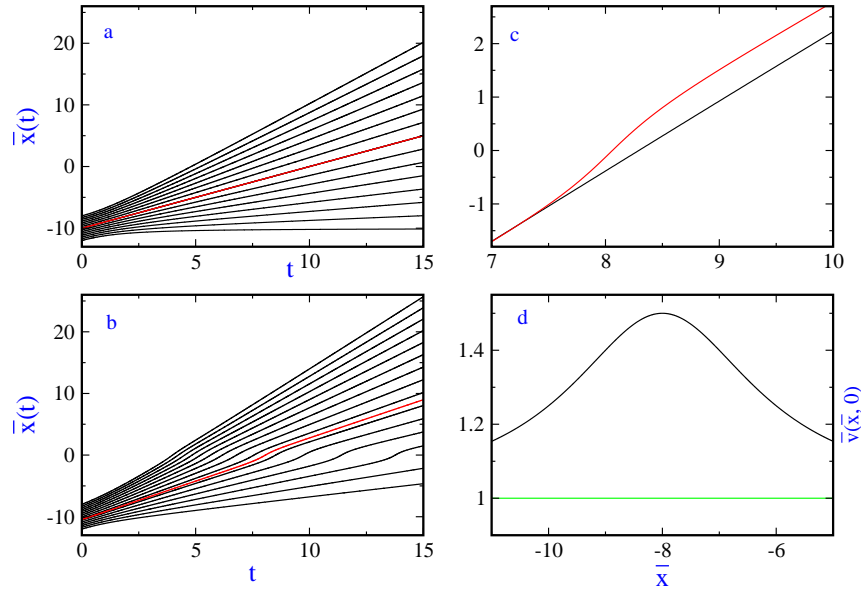


FIG. 4: (Color online) A selection of Bohmian trajectories for free Gaussian wavepacket (a) and interacting nonreflecting wavepacket (b). In both plots (a) and (b) red trajectory starts at  $\langle \bar{x} \rangle(0)$ . In plot (c) black curve shows  $\langle \bar{x} \rangle(t)$  for the interacting nonreflecting wavepacket and the red one represents the Bohm trajectory with initial position  $\langle \bar{x} \rangle(0)$ . In plot (d) one sees initial Bohmian velocity as a function of  $\bar{x}$  for nonreflecting interacting wavepacket (black curve) and for free Gaussian packet (green curve).

- [15] C. R. Leavens, *Phys. Lett. A* **178** (1993) 27.
- [16] J. Finkelstein, *Phys. Rev. A* **59** (1999) 3218.
- [17] D. J. Griffiths 1995, *Introduction to Quantum Mechanics* (New Jersey: Prentice-Hall), p: 72, Problem 2.48.
- [18] C. Grosche, F. Steiner 1998, *Handbook of Feynman Path Integrals* (Springer Tracts in Modern Physics, Vol. 145), p: 246, eq. (6.6.12).
- [19] D. Dürr, S. Goldstein and N. Zangh, *J. Stat. Phys.* **67** (1992) 843.
- [20] B. Thaller 2000, *Visual Quantum Mechanics* (New York: Springer-Verlag), p: 53, Sec. 3.1.3.